Multigrid Solutions Of The Euler And Navier-Stokes Equations For A Series 60 Cb = 0.6 Ship Hull For Froude Numbers 0.160, 0.220 And 0.316 Program 1: Navier-Stokes Formulation Program 2: Euler Formulation*

J. Farmer† L. Martinelli‡

A. Jameson§

Department of Mechanical and Aerospace Engineering
Princeton University
Princeton, New Jersey 08544

*Paper presented at the CFD Workshop Tokyo, Tokyo, Japan, 22-25 March 1994.

†Research Associate

‡Research Staff Member

§Professor

Multigrid Solutions Of The Euler And Navier-Stokes Equations For A Series 60 Cb = 0.6 Ship Hull For Froude Numbers 0.160, 0.220 And 0.316 (Program 1: Navier-Stokes Formulation)*

J. Farmer† L. Martinelli‡

A. Jameson§

Department of Mechanical and Aerospace Engineering
Princeton University
Princeton, New Jersey 08544

Summary

This paper presents the modifications to the Euler method which are incorporated to obtain viscous Navier-Stokes solutions to the ship wave problem. The discussion pertaining to this formulation is limited to the viscous discretization and turbulence model, additional details concerning the flow solver may be found in Program 2. Comparisons between the Euler and Navier-Stokes results are made at the end of this paper.

1 Introduction

There are times when an inviscid calculation is sufficient to yield the data required from a flow simulation about a ship hull. This is particularly true if only information such as the wave drag experienced by a translating ship is needed (see discussion in companion paper). However, if information such as flow separation in the stern region of a ship and its influence on the resulting wave and friction drag is required, one must resort to viscous calculations [1, 2]. Therefore, the general direction of this portion of the paper is to build upon the Euler formulation presented in Program 2 and present a fast and robust method for the computation of viscous flow about ship hulls with associated free surface effects.

2 Mathematical Model

Figure 1 shows the reference frame and ship location used in this work. A right-handed coordinate system $Oxyz$, with the origin fixed at midship on the mean free surface is established. The z direction is positive upwards, y is positive towards the starboard side and x is positive in the aft direction. The free stream velocity vector is parallel to the x axis and points in the same direction. The ship hull pierces the uniform flow and is held fixed in place, ie. the ship is not allowed to sink (translate in z direction) or trim (rotate in $x-z$ plane).

*Paper presented for Program 1 at the CFD Workshop Tokyo, Tokyo, Japan, 22-25 March 1994.
†Research Associate
‡Research Staff Member
§Professor

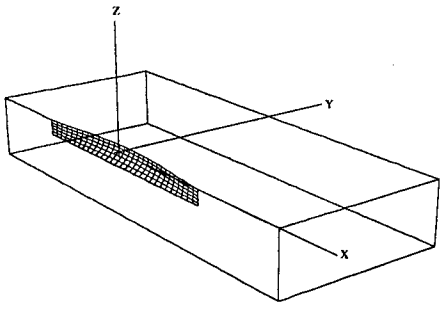

Figure 1: Reference Frame and Ship Location

2.1 Bulk Flow

For a viscous incompressible fluid moving under the influence of gravity, the continuity equation and the Reynolds averaged Navier-Stokes equations may be put in the form [3],

$$u_x + v_y + w_z = 0 \tag{1}$$

$$\begin{aligned} u_t + uu_x + vu_y + wu_z &= -\psi_x + \left(Re^{-1} + \nu_t\right)\left(\nabla^2 u\right) \\ v_t + uv_x + vv_y + wv_z &= -\psi_y + \left(Re^{-1} + \nu_t\right)\left(\nabla^2 v\right) \\ w_t + uw_x + vw_y + ww_z &= -\psi_z + \left(Re^{-1} + \nu_t\right)\left(\nabla^2 w\right). \end{aligned} \tag{2}$$

Here, $u = u(x, y, z, t)$, $v = v(x, y, z, t)$ and $w = w(x, y, z, t)$ are the mean total velocity components in the x, y and z directions. All lengths and velocities are nondimensionalized by the ship length L and the free stream velocity U, respectively. The pressure ψ is the static pressure p minus the hydrostatic component $-zFr^{-2}$ and may be expressed as $\psi = p + zFr^{-2}$, where $Fr = \frac{U}{\sqrt{gL}}$ is the Froude number. The pressure variable ψ is nondimensionalized by ρU^2. The Reynolds number Re is defined by $Re = \frac{UL}{\nu}$ where ν is the kinematic viscosity of water and is constant. ν_t is the dimensionless turbulent eddy viscosity, computed locally using the Baldwin-Lomax turbulence model. This set of equations shall be solved subject to the following boundary conditions.

2.2 Boundary Conditions

2.2.1 Free Surface

The free surface boundary conditions used for the Navier-Stokes model are the same as those used in the Euler model and are repeated here for discussion in this paper:

$$p = constant$$

$$\frac{d\beta}{dt} = w = \beta_t + u\beta_x + v\beta_y \tag{3}$$

where $z = \beta(x, y, t)$ is the free surface location.

2.2.2 Hull and Farfield

On the hull the condition is that of no-slip and is stated as

$$u = v = w = 0.$$

All the farfield and symmetry plane boundary conditions are the same as those outlined in Program 2.

2.3 Turbulence Model

To model turbulence in the flow field the laminar viscosity is replaced by

$$\mu = \mu_l + \mu_t$$

where the turbulent viscosity μ_t is computed using the algebraic model of Baldwin and Lomax [4]. The Baldwin-Lomax model is an algebraic scheme that makes use of a two-layer, isotropic eddy viscosity formulation. The model performs well for problems which do not exhibit large regions of separated flow and appears to be sufficient for the class of problems addressed in the present work. In this model the turbulent viscosity is evaluated using

$$\mu_t = \begin{cases} (\mu_t)_{inner} & y \leq y_{crossover} \\ (\mu_t)_{outer} & y > y_{crossover} \end{cases}$$

where y is the distance measured normal to the body surface and $y_{crossover}$ is the minimum value of y where both the inner and outer viscosities match. The inner viscosity follows the Prandtl-Van Driest formula,

$$(\mu_t)_{inner} = l^2|\omega|$$

where

$$l = ky\left[1 - exp(-y^+/A^+)\right]$$

is the turbulent length scale for the inner region, k and A^+ are model constants, $|\omega|$ is the vorticity magnitude and $y^+ = (\tau_w/\mu_w)y$ is the dimensionless distance to the wall in wall units.

In the outer region of the boundary layer, the turbulent viscosity is given by

$$(\mu_t)_{outer} = KC_{cp}F_{wake}F_{Kleb}$$

where K and C_{cp} are model constants, the function F_{wake} is

$$F_{wake} = min\left(y_{max}F_{max}, C_{wk}y_{max}U_{dif}^2/F_{max}\right)$$

and the function F_{Kleb} is

$$F_{Kleb} = \left[1 + 5.5\left(\frac{C_{Kleb}y}{y_{max}}\right)^6\right]^{-1}.$$

The quantities F_{max} and y_{max} are determined by the value and corresponding location, respectively, of the maximum of the function

$$F = y|\omega|\left[1 - exp(-y^+/A^+)\right].$$

The quantity U_{dif} is the difference between maximum and minimum velocity magnitudes in the profile and is expressed as

$$U_{dif} = (u^2 + v^2 + w^2)_{max}^{1/2} - (u^2 + v^2 + w^2)_{min}^{1/2}$$

C_{Kleb} and C_{wk} are additional model constants. Numerical values for the model constants used in the computations are listed here:

$$A^+ = 26,\ k = 0.4,\ K = 0.0168,$$

and

$$C_{cp} = 1.6,\ C_{wk} = 1.0,\ C_{Kleb} = 0.3.$$

3 Numerical Solution

The numerical solution follows essentially that outlined in the Euler method. The only major difference is the inclusion of the viscous fluxes, whose discretization is discussed later in this section. The viscous counterpart of the numerical solution is given here.

3.1 Bulk Flow Solution

The governing set of incompressible flow equations may be written in vector form as

$$\mathbf{w}_{t^*} + (\mathbf{f} - \mathbf{f_V})_x + (\mathbf{g} - \mathbf{g_V})_y + (\mathbf{h} - \mathbf{h_V})_z = 0 \tag{4}$$

where the vector of dependent variables $\mathbf{w}$ and inviscid flux vectors $\mathbf{f}$, $\mathbf{g}$ and $\mathbf{h}$ are identical to those listed in Program 2. The viscous flux vectors $\mathbf{f_V}$, $\mathbf{g_V}$ and $\mathbf{h_V}$ are given by

$$\begin{aligned} \mathbf{f_V} &= [0,\ \tau_{xx},\ \tau_{xy},\ \tau_{xz}]^T \\ \mathbf{g_V} &= [0,\ \tau_{yx},\ \tau_{yy},\ \tau_{yz}]^T \\ \mathbf{h_V} &= [0,\ \tau_{zx},\ \tau_{zy},\ \tau_{zz}]^T \end{aligned}$$

where the viscous stress components are defined as

$$\begin{aligned} \tau_{xx} &= (Re^{-1} + \nu_t)(2u_x - 2/3(u_x + v_y + w_z)) \\ \tau_{yy} &= (Re^{-1} + \nu_t)(2v_y - 2/3(u_x + v_y + w_z)) \\ \tau_{zz} &= (Re^{-1} + \nu_t)(2w_z - 2/3(u_x + v_y + w_z)) \\ \tau_{xy} &= (Re^{-1} + \nu_t)(u_y + v_x) \\ \tau_{yz} &= (Re^{-1} + \nu_t)(v_z + w_y) \\ \tau_{zx} &= (Re^{-1} + \nu_t)(w_x + u_z). \end{aligned}$$

The same discussion regarding the artificial compressibility in Program 2 applies here. However it should be noted that a cutoff value of Γ will be activated in the viscous boundary layer near the hull to prevent Γ from becoming zero or nearly so.

Following the general procedures for FVM, the governing equations may be integrated over an arbitrary volume Λ. Application of the divergence theorem on the convective and viscous flux term integrals yields

$$\frac{\partial}{\partial t^*}\int_\Lambda \mathbf{w}d\Lambda + \int_{\partial\Lambda}(\mathbf{f}dS_x + \mathbf{g}dS_y + \mathbf{h}dS_z) - \int_{\partial\Lambda}(\mathbf{f_V}dS_x + \mathbf{g_V}dS_y + \mathbf{h_V}dS_z) = 0$$

where S_x, S_y and S_z are the projected areas in the x, y and z directions, respectively. The computational domain is divided into hexahedral cells. Application of FVM to each of the computational cells results in the following system of ordinary differential equations,

$$\frac{d}{dt^*}(\Lambda_{ijk}\mathbf{w}) + C_{ijk} - V_{ijk} = 0.$$

The volume Λ_{ijk} is given by the summation of the eight cells surrounding node i,j,k. The convective flux $C_{ijk}(\mathbf{w})$ is defined as

$$C_{ijk}(\mathbf{w}) = \sum_{k=1}^{n}(\mathbf{f}S_x + \mathbf{g}S_y + \mathbf{h}S_z)_k \tag{5}$$

and the viscous flux $V_{ijk}(\mathbf{w})$ is defined as

$$V_{ijk}(\mathbf{w}) = \sum_{k=1}^{n}(\mathbf{f_V}S_x + \mathbf{g_V}S_y + \mathbf{h_V}S_z)_k \tag{6}$$

where the summation is over the n faces surrounding Λ_{ijk}.

The discretization for the viscous fluxes follows the guidelines originally proposed in [5, 6] for the simulation of two dimensional viscous flows. The components of the stress tensor are computed at the cell centers with the aid of Gauss' formula. The viscous fluxes are then computed by making use of an auxiliary cell bounded by the faces lying on the planes containing the centers of the cells surrounding

a given vertex and the mid-lines of the cell faces. For example, the u_x term in τ_{xx} may be computed from

$$u_x \Lambda = \int_\Lambda u_x d\Lambda = \int_{\partial\Lambda} u d\partial\Lambda_x \approx \sum_{k=1}^{6} u_k S_{x_k}$$

where $k = 1,6$ are the six faces surrounding a particular cell, u_k is an average of the velocities from the nodes that define the k^{th} face and S_{x_k} are the projected areas in the x direction corresponding to each face. Once the components of the complete stress tensor are computed at the centroids of the cells then the same method of evaluation may be used to compute the viscous fluxes at the vertex through use of equation 6. For this purpose the control volume is now constructed by assembling $\frac{1}{8}$ fractions of each of the eight cells surrounding a particular vertex. The equivalent two dimensional control volume is sketched in the figure below. This discretization procedure is designed to minimize the error induced

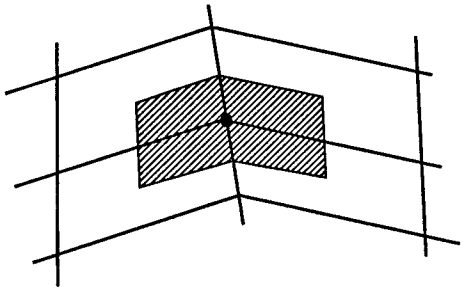

by a kink in the grid. It has proved to be accurate and efficient in applications to the solution of three dimensional compressible viscous flows [7, 8].

The discretized set of equations are solved in exactly the same way as outlined in Program 2. An explicit time integration is used to solve the Navier-Stokes discretization with artificial dissipation added to prevent decoupling. The multigrid method is used to accelerate convergence.

3.2 Free Surface Solution

The free surface update procedure follows essentially the same lines as those presented in Program 2. However, for the Navier-Stokes equations the no-slip boundary condition is inconsistent with the free surface boundary condition at the hull/waterline intersection. To circumvent this difficulty the computed elevation for the second row of grid points away from the hull is extrapolated to the hull. Since the minimum spacing normal to the hull is small, the error due to this should be correspondingly small, comparable with other discretization errors. The treatment of this intersection for the Navier-Stokes calculations, should be the subject of future research to find the most accurate possible procedure.

4 Results

4.1 Computational Conditions

Figure 2 shows a portion of the fine grid resulting from the Navier-Stokes calculation. The number of grid points is 193, 65 and 49 in the x, y and z-directions respectively, and the $H-H$ type grid is used. The resolution on the hull surface is 97 by 25. The grid extends 1 ship length upstream from the bow, $2\frac{1}{2}$ ship lengths downstream from the stern, 2 ship lengths to starboard, and 1 ship length down below the undisturbed free surface. Grid points are clustered near the bow and stern with a minimum spacing of 0.005 dimensionless units based on the hull length. The minimum spacing in the y-direction, normal to the hull surface, is 0.00002 for the Navier-Stokes computations. The number of grid points in the y-direction is increased to 65 to provide resolution of the boundary layer. This resulted in y^+ values

for the first cell normal to the hull to reside in the range $.75 < y^+ < 1.5$ and $1.5 < y^+ < 3.0$ for the $Re = 2.0E + 6$ and $Re = 4.0E + 6$ cases, respectively.

4.2 Series 60, $C_b = 0.6$ Hull

Simulations were run for three Froude numbers: 0.160, 0.220 and 0.316. These are the same cases which were run for Program 2 and the overhead wave profiles are compared in figures 3, 4 and 5. The degree of similarity between the computed Euler and Navier-Stokes simulations is rather striking. Only in the stern region and aft is there major differences in the wave patterns. This is most likely due to displacement effects and flow separation in the Navier-Stokes results.

Figure 6 presents the computed wave elevation profiles along the hull, the residuary drag, the friction drag and the total drag. [1] The experimental data for the wave profiles was measured from the data presented in [9] for Froude numbers equal to 0.160 and 0.316 and data obtained from SRI in Japan for Froude number equal 0.220.

The computational times for the simulations are approximately 30 and 45 hours for the Euler and Navier-Stokes calculations, respectively, using a single processor Convex 220 computer with 64-bit arithmetic. The Euler simulations consist of 500 steps on a $25 \times 7 \times 7$ grid, 500 steps on a $49 \times 13 \times 13$ grid, 500 steps on a $97 \times 25 \times 25$ grid and 500 steps on a $193 \times 49 \times 49$ grid. The Navier-Stokes simulations consist of 500 steps on a $25 \times 9 \times 7$ grid, 500 steps on a $49 \times 17 \times 13$ grid, 500 steps on a $97 \times 33 \times 25$ grid and 500 steps on a $193 \times 65 \times 49$ grid. It is important to point out that approximately ten percent of the total CPU time for the simulation has been used by step 1500 (refer to figure 6). The remaining ninety percent of the CPU time is used to compute the fine grid solution and a good indication of the final result is obtained well before 500 steps on the fine grid have been reached. For the given resolution these CPU times appear to represent about a ten-fold decrease in the CPU times reported in the earlier literature, which have usually been presented for coarser grids. The CPU time required for the free surface update and regriding procedures is approximately seven percent that required for the bulk flow calculations.

5 Conclusions

The objective of the this work was to present an efficient method to compute Euler and Navier-Stokes solutions for the nonlinear ship wave problem. It appears from the results presented that good predictions of the wave pattern and associated drag can be achieved using the Euler flow model without the added complexity required for the viscous solution. This is encouraging since the Euler simulations can be performed using less computer time and a fraction of the computer memory than the Navier-Stokes simulations require. However, for problems which demand that the interaction between the viscous boundary layer and wave making be coupled, the formulation presented herein can be used to efficiently compute the solution.

Acknowledgment

The authors gratefully appreciate the contribution of James Reuther (NASA-Ames) for his time and effort spent helping construct the grids used for the Series 60 hull. Our work has benefited greatly from the support of the Office of Naval Research through Grant N00014-93-I-0079, under the supervision of Dr. E.P. Rood.

References

[1] Toda,Y., Stern,F., and Longo,J., "Mean-Flow Measurements in the Boundary Layer and Wake and Wave Field of a Series 60 $C_B = 0.6$ Ship Model–Part1: Froude Numbers 0.16 and 0.316," *Journal of Ship Research*, v. 36, n. 4, pp. 360-377, 1992.

[1] The residuary drag is computed by integrating the pressure over the hull surface in exactly the same fashion as the wave drag is computed in the Euler formulation. It is referred to as residuary drag in this case to make the distinction from pure wave drag which can be computed through pressure integration in the Euler formulation.

[2] Longo,J., Stern,F., and Toda,Y., "Mean-Flow Measurements in the Boundary Layer and Wake and Wave Field of a Series 60 $C_B = 0.6$ Ship Model–Part2: Effects on Near-Field Wave Patterns and Comparisons with Inviscid Theory," *Journal of Ship Research,* v. 37, n. 1, pp. 16-24, 1993.

[3] Hino,T., "Computation of Free Surface Flow Around an Advancing Ship by the Navier-Stokes Equations," *Proceedings, Fifth International Conference on Numerical Ship Hydrodynamics,* pp. 103-117, 1989.

[4] Baldwin,B.S., and Lomax,H., "Thin Layer Approximation and Algebraic Model for Separated Turbulent Flows," *AIAA Paper 78-257, AIAA 16th Aerospace Sciences Meeting,* Reno, NV, January 1978.

[5] Martinelli,L., "Calculations of Viscous Flows with a Multigrid Method," Ph.D. Thesis, MAE T-1754, Princeton University, 1987.

[6] Martinelli,L. and Jameson,A., "Validation of a Multigrid Method for the Reynolds Averaged Equations," *AIAA Paper 88-0414, AIAA 26st Aerospace Sciences Meeting,* Reno, NV, January 1988.

[7] Liu,F. and Jameson,A., "Multigrid Navier-Stokes Calculations For Three-Dimensional Cascades," *AIAA Paper 92-0190, AIAA 30th Aerospace Sciences Meeting,* Reno, NV, January 1990.

[8] Martinelli,L., Jameson,A., and Malfa,E., "Numerical Simulation of Three-Dimensional Vortex Flows Over Delta Wing Configurations," *Lecture Notes in Physics, Volume 414. Thirteenth International Conference on Numerical Methods in Fluid Dynamics,*. M. Napolitano and F. Sabetta (Eds.), Rome, Italy, 1992.

[9] Toda,Y., Stern,F., and Longo,J., "Mean-Flow Measurements in the Boundary Layer and Wake and Wave Field of a Series 60 $C_B = 0.6$ Ship Model for Froude Numbers .16 and .316," IIHR Report No. 352, Iowa Institute of Hydraulic Research, The University of Iowa, Iowa City, Iowa, 1991.

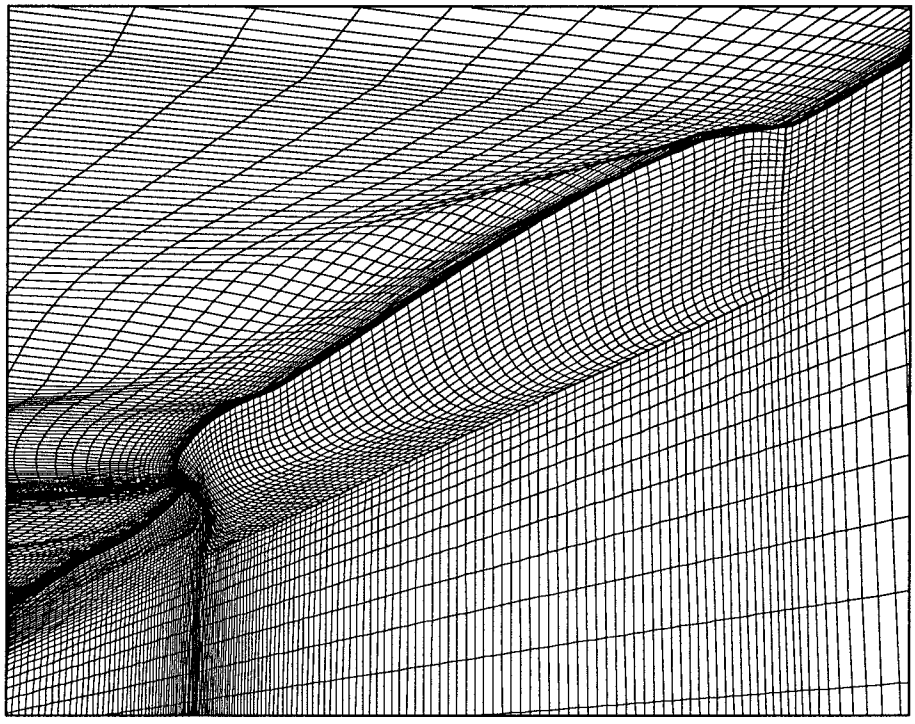

Figure 2: Final Distorted Fine Grid for Series 60, Cb = 0.6, Fr = 0.316

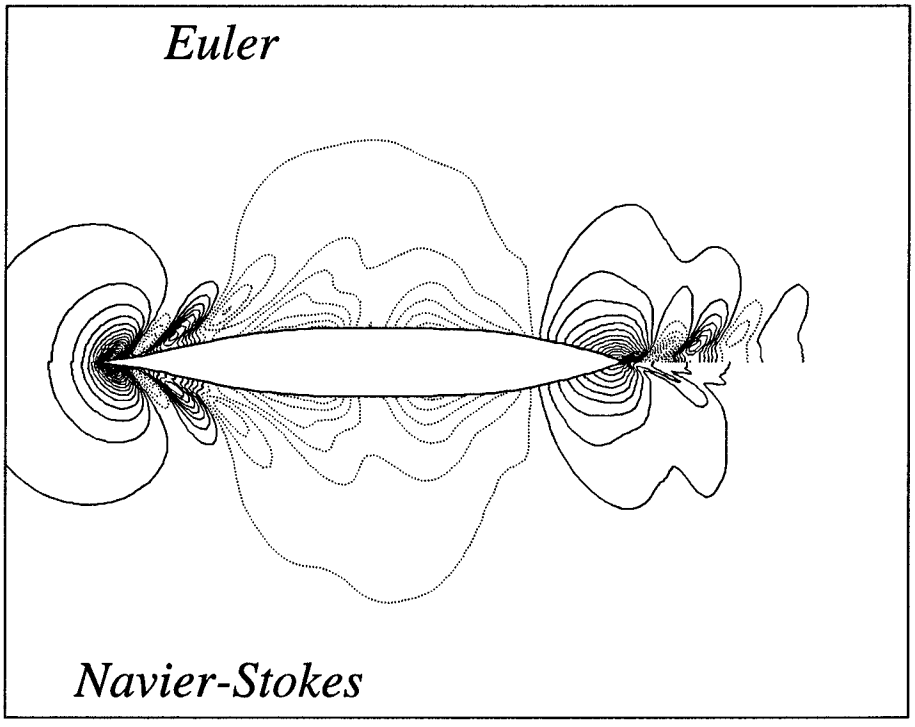

Figure 3: Comparison of Computed Overhead Wave Profiles, Fr = 0.160

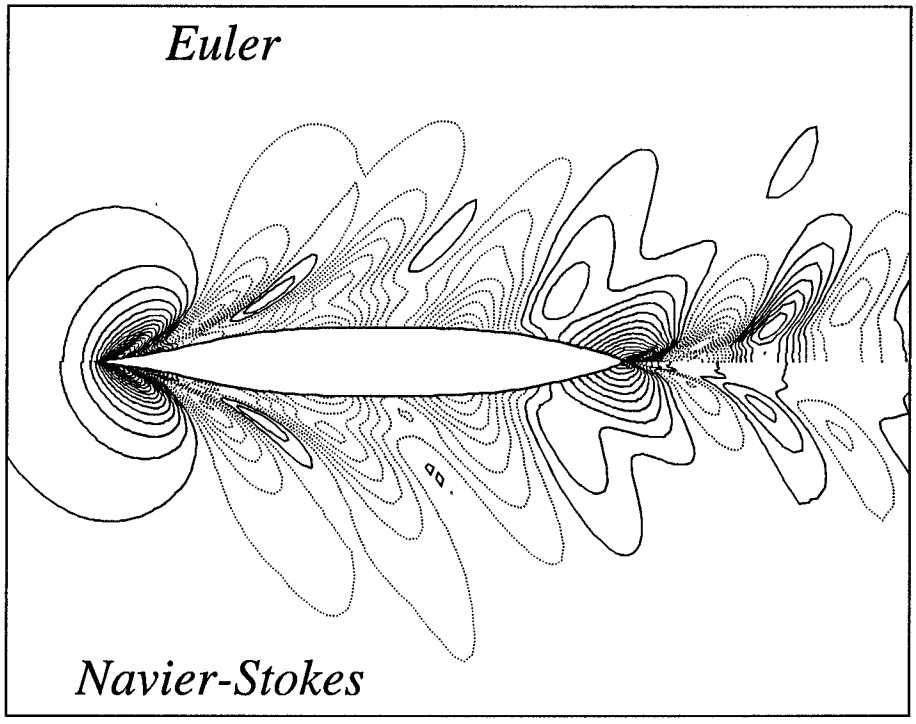

Figure 4: Comparison of Computed Overhead Wave Profiles, Fr = 0.220

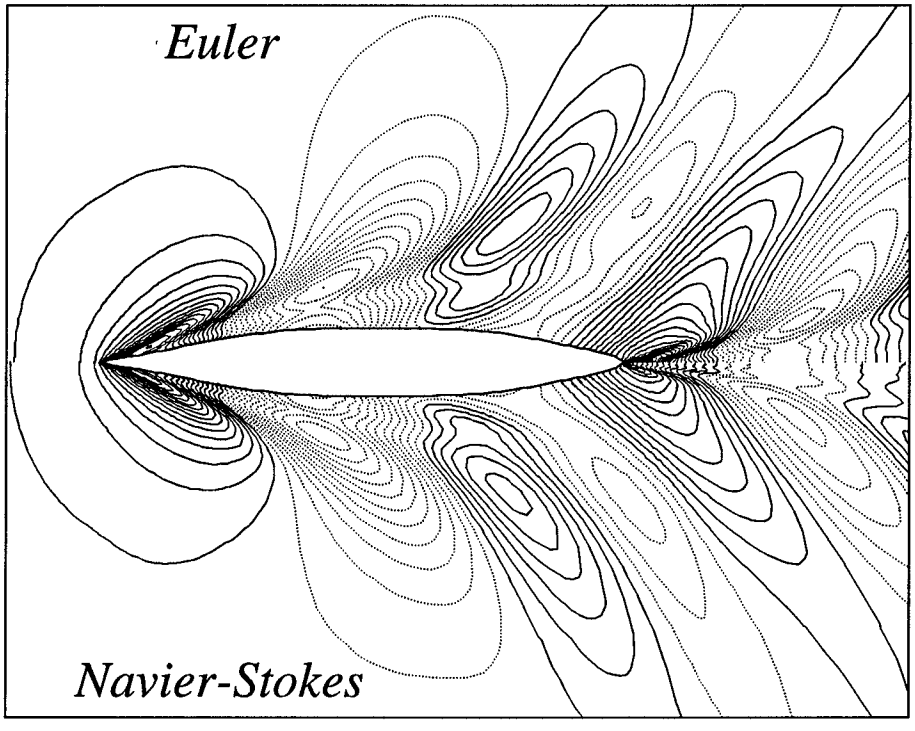

Figure 5: Comparison of Computed Overhead Wave Profiles, Fr = 0.316

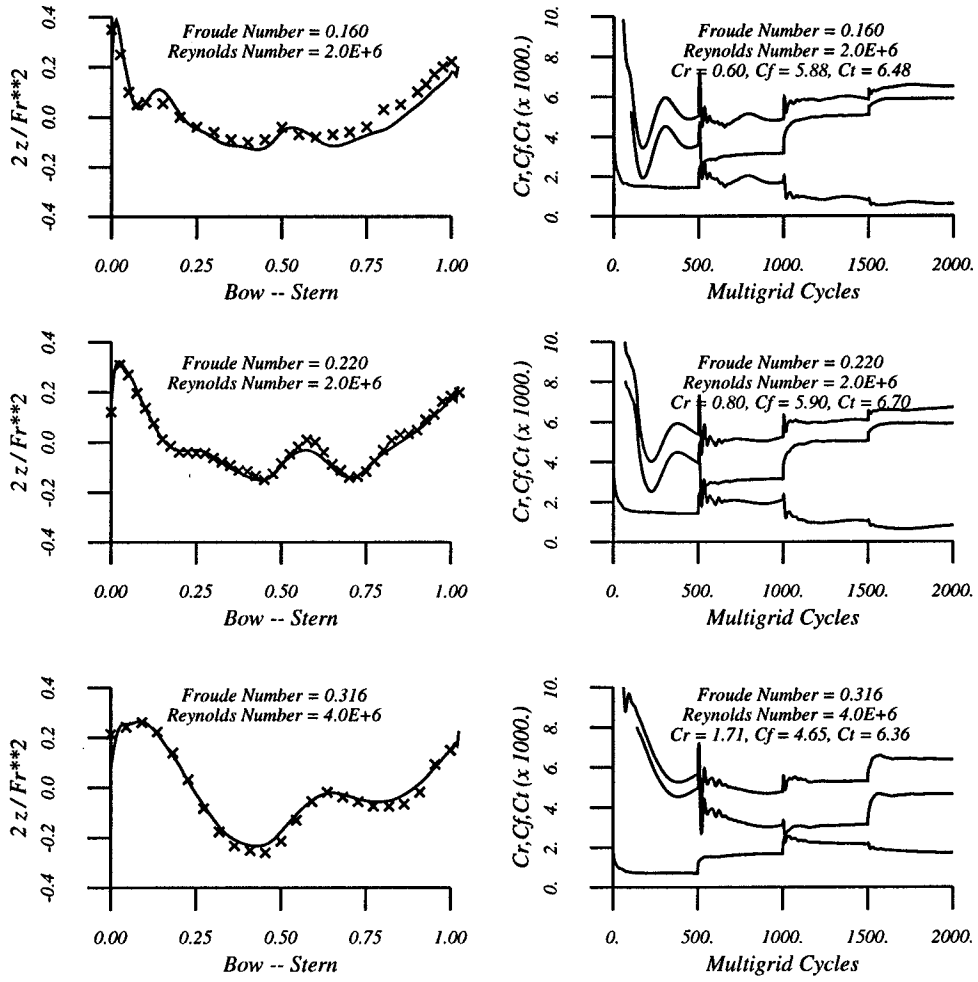

Navier Stokes Calculations
Series 60, Cb=0.60
Grid #1: Cycles 000-500, (25 x 9 x 7)
Grid #2: Cycles 501-1000, (49 x 17 x 13)
Grid #3: Cycles 1001-1500, (97 x 33 x 25)
Grid #4: Cycles 1501-2000, (193 x 65 x 49)
Delta y for Grid #4, 2.0E-5

Figure 6: Hull Wave Profiles and Drag History